communications biology

A Nature Portfolio journal

Article

https://doi.org/10.1038/s42003-025-08035-6

Stk24 deficiency causes disrupted hippocampal neurogenesis and anxiety-like behavior in mice

Kuan-Yu Wu [1,4], Chi-Hui Tsao[1,4], Nicole Ching Su[1], Shin-Meng Deng [1] & Guo-Jen Huang [1,2,3]

Protein kinases regulate protein activity through phosphorylation, and many have been reported to participate in brain development. Among them, serine/threonine-protein kinase 24 (STK24) is believed to influence apoptosis, spinal synaptogenesis, and neuronal migration. Despite its recognized roles, the functions of STK24 in the brain remains insufficiently explored. Here, we present an in vivo study of brain-specific *Stk24* conditional knockout mice. We investigate the impact of *Stk24* deletion through histological analysis, behavior assays, and the molecular changes. In our results, *Stk24* deletion disrupts the hippocampal formation during development and decreased subsequent adult hippocampal neurogenesis whilst neuronal morphology is relatively unaffected. Additionally, *Stk24*-deficient mice exhibit anxiety-like behavior and altered stress responses, featuring increased hippocampal neuronal activity, dysregulated HPA axis reactivity, and modified expression patterns of glucocorticoid receptor signaling-related genes. In conclusion, our findings highlight the involvement of *Stk24* in brain development, adult hippocampal neurogenesis, as well as anxiety and stress responses.

Protein kinases regulate the biological activity of proteins via phosphorylation. It has been reported that numerous kinases participate in brain development including promoting axonal growth and altering neurogenesis. Serine/Threonine-protein kinase 24 (STK24), also known as Mammalian sterile 20-like kinase-3 (MST3), is one of those kinases. It is well known for its role as an upstream regulator of the mitogen-activated protein kinase (MAPK) signaling pathway, mediating multiple biological processes including apoptosis, morphogenesis, and cell migration[1]. The encoded protein, MST3, consists of a shorter MST3a and a longer MST3b isoform, which differ by 12 amino acids[2]. MST3a is expressed universally and is believed to regulate apoptosis and neuronal migration during brain development[3]. MST3b, demonstrated to participate in axonal outgrowth, is selectively expressed in the brain; particularly highly in the hippocampus and cerebral cortex[2,4]. According to the Hippocampus RNA-seq Atlas (https://hipposeq.janelia.org), *Stk24* is expressed throughout the dorsal and ventral hippocampus with equivalent expressions in CA1, CA2, CA3, and DG regions. Additionally, as reported by the Human Protein Atlas (https://www.proteinatlas.org), STK24/MST3 is expressed in excitatory neurons, inhibitory neurons, and glial cells.

So far, many studies have revealed the impact of STK24/MST3 on the central nervous system. Among them, it is reported that shRNA-induced *Stk24* silencing reduced spinal synapses but increased filopodia in developing hippocampal cultures[5]. *In utero* silencing of *Stk24* also disrupted neuronal positioning and dendritogenesis by modulating RhoA activity in mice[6]. Moreover, knocking down *Stk24* in rat dorsal root ganglions was shown to severely impair the regeneration of injured axons[7]. Previous studies have provided new insight into the role of *Stk24* in brain development. However, most of them used shRNA to evaluate the roles of *Stk24* in neuronal cells. The influence of *Stk24* deletion on the brain and animal behavior is currently lacking. Here, we present an in vivo study of brain-specific *Stk24* conditional KO (cKO) mice to reveal the roles of *Stk24* in the brain, ranging from histological analysis to behavioral phenotypes. Our results showed that brain-specific *Stk24* cKO mice exhibited ectopic neurons in the hippocampus during brain development, along with impaired adult hippocampal neurogenesis. Increased anxiety and elevated stress-induced plasma corticosterone were also discovered. Our study demonstrates that *Stk24* plays a role in hippocampal architecture and mediates animal behavior.

[1]Graduate Institute of Biomedical Sciences, College of Medicine, Chang Gung University, Taoyuan, 333, Taiwan. [2]Department of Biomedical Sciences, College of Medicine, Chang Gung University, Taoyuan, 333, Taiwan. [3]Neuroscience Research Center, Chang Gung Memorial Hospital at Linkou, Taoyuan, 333, Taiwan. [4]These authors contributed equally: Kuan-Yu Wu, Chi-Hui Tsao. e-mail: gjh30@mail.cgu.edu.tw

Results

Brain-specific conditional knockout of *Stk24* disrupted postnatal hippocampal development

A brain-specific *Stk24* conditional knockout (cKO) mouse model was generated by crossing *Stk24* floxed mice with *Sox1*::*Cre* mice, which express *Cre* throughout the neural tube from E9.5[8,9]. This conditional knockout model allowed us to investigate the functions of *Stk24* in the brain. Knockout efficiency was validated at both the mRNA and protein levels using real-time PCR and western blot, respectively, both of which showed a significant reduction in *Stk24* expression compared to the control wild-type (WT) group (PCR: $t_{(16)} = 10.37$, $p < 0.001$; western blot: $t_{(4)} = 4.88$, $p < 0.01$) (Fig. 1a). The specificity of this conditional knockout model was confirmed by the significant reduction of *Stk24* in the brain, while the peripheral regions such as liver levels remained unchanged (OB: mRNA $t_{(5)} = 10.73$, $p = 0.001$; Protein $t_{(5)} = 5.58$, $p < 0.01$; CTX: mRNA $t_{(6)} = 8.80$, $p < 0.001$; Protein $t_{(5)} = 7.12$, $p < 0.001$; HIP: mRNA $t_{(6)} = 14.66$, $p < 0.001$; Protein $t_{(5)} = 7.05$, $p < 0.001$; THAL: mRNA $t_{(6)} = 6.68$, $p < 0.001$; Protein $t_{(4)} = 8.06$, $p < 0.01$; CB: mRNA $t_{(6)} = 9.46$, $p < 0.001$; Protein $t_{(5)} = 8.55$, $p < 0.001$; Liver: mRNA $t_{(6)} = 0.44$, $p = 0.67$; Protein $t_{(5)} = 1.59$, $p = 0.17$) (Supplementary Fig. 1).

Since *Stk24* is known to influence synaptic morphology in developing hippocampal cultures[5], we first asked whether *Stk24* deletion affected the neuronal outgrowth and postnatal neurogenesis in developing brains. To this end, Golgi staining was performed on postnatal day 13 (p13) mouse brains to examine the morphology of hippocampal neurons. Dendritic spine density was quantified, and there was no significant difference in the densities between the groups ($t_{(6)} = 1.28$, $p = 0.24$) (Fig. 1b). We further conducted Sholl analysis for a more detailed investigation, and our results showed that WT and *Stk24* cKO mice exhibited equivalent dendritic branching ($F_{(1,18)} = 0.44$, $p = 0.51$), total intersections ($t_{(18)} = 0.66$, $p = 0.51$), and length of the longest dendrite ($t_{(18)} = 1.83$, $p = 0.08$) (Fig. 1c), suggesting unaffected neuronal morphology in the absence of *Stk24*. Next, we studied the postnatal neurogenesis by assessing the expression of neurogenesis markers including PAX6, TBR2, NeuroD, and PROX1. Immunohistochemical (IHC) staining was performed on p13 mouse brains, and the result showed disrupted hippocampal neurogenesis in *Stk24* cKO mice, featuring ectopic granule cells in the DG of the hippocampus (Fig. 1d). Given that hippocampal neurogenesis occurs in the sub-granular layer of the DG under normal conditions, we calculated the antibody-labeled cells in the hilus for the quantification of ectopic cells, and there was an overall significant increase in *Stk24* cKO group (PAX6: $t_{(6)} = 4.61$, $p < 0.01$; TBR2: $t_{(6)} = 5.15$, $p < 0.01$; NeuroD: $t_{(2)} = 13.16$, $p < 0.01$; PROX1: $t_{(6)} = 7.93$, $p < 0.001$). Taken together, despite unaffected neuronal morphology, *Stk24* deletion disrupted hippocampal neurogenesis during brain development.

To investigate gene expression differences between WT and cKO mice, we performed RNA-sequencing on hippocampal tissues from P13 mice. Differential expression analysis was conducted using DESeq2, with the following criteria for identifying differentially expressed (DE) genes: *p*-value < 0.05; |Log2 fold change (FC)| >0.5; baseMean >20. A total of 114 DE genes were identified, of which 74 were significantly up-regulated and 40 were down-regulated (Fig. 1e). Gene ontology (GO) enrichment analysis was further conducted via WebGestalt (https://www.webgestalt.org, accessed on 2025-02-11) focusing on biological process (BP). This analysis revealed 10 up-regulated and 8 down-regulated pathways from these DE genes (Fig. 1f). The enriched GO categories compassed a broad range of biological processes including hormone response, differentiation and development, cell division, apoptosis and autophagy. Interestingly, the down-regulated genes were strongly associated with neurogenesis, neuron migration, and pattern specification, which is in line with our previous results where *Stk24* cKO mice exhibited disrupted postnatal neurogenesis and hippocampal formation.

Moreover, since *Stk24* is well recognized for its role as an upstream regulator of the MAPK signaling pathway, we specifically examined the expression of MAPK pathway-related genes[1]. The gene list was obtained from the mouse gene set "MAPK Family Signaling Cascades" (R-MMU-5683057), provided by the Reactome database through the Molecular Signatures Database (MSigDB) (https://www.gsea-msigdb.org, accessed on 2025-02-12). Among the 303 MAPK pathway-related genes, 27 genes (12 up-regulated genes and 15 down-regulated genes) exhibited significant expression changes with a *p*-value < 0.05 (Supplementary Fig. 2a). However, when we further conducted the Kyoto Encyclopedia of Genes and Genomes (KEGG) pathway enrichment analysis via WebGestalt (https://www.webgestalt.org, accessed on 2025-02-11) using gene set enrichment analysis (GSEA), MAPK pathway was not targeted as a significantly enriched pathway (Supplementary Fig. 2b). In summary, although several MAPK pathway-related genes were significantly affected by *Stk24* deletion, the overall MAPK signaling pathway did not appear to be influenced. It indicated that MAPK pathway may not be the major pathway affected by *Stk24* knockout, or the genetic expression changes was not sufficient to impact the pathway-level regulation.

Brain-specific *Stk24* cKO mice exhibited hyperactivity and increased anxiety

Deletion of *Stk24* was demonstrated to affect the hippocampal development. Since the hippocampal formation is widely believed to be involved in emotional responses and cognitive abilities[10], we further investigated the effects of *Stk24* on animal behaviors, particularly those related to the hippocampal functions. Before the mice were subjected to a series of behavioral tests, the spontaneous locomotor activity was assessed. *Stk24* cKO mice displayed a significantly longer travel distance as compared to WT mice during active phase ($F_{(1,26)} = 8.80$, $p < 0.01$), but not inactive phase ($F_{(1,26)} = 0.07$, $p = 0.78$), suggesting a tendency to hyperactivity (Fig. 2a). Grip strength and motor coordination were also measured by grip test and rotarod test, respectively. Both showed no significant difference between the groups (grip: $t_{(26)} = 1.60$, $p = 0.12$; rotarod: $t_{(26)} = 1.32$, $p = 0.19$), suggesting normal motor skills (Supplementary Fig. 3a, b).

Open field, elevated O-maze, and the light-dark box were used to evaluate anxiety in mice. Although there was no significant difference in the results of the elevated O-maze (relative distance: $t_{(26)} = 1.41$, $p = 0.17$; duration: $t_{(26)} = 1.10$, $p = 0.27$; transition: $t_{(26)} = 1.07$, $p = 0.29$) (Fig. 2c; Supplementary Fig. 3d), both of the open field and light-dark box tests showed remarkable differences between cKO and control WT group. In open field test, despite equivalent relative distance in the center zone ($t_{(26)} = 1.72$, $p = 0.09$), *Stk24* cKO mice exhibited less time in the center area ($t_{(26)} = 2.09$, $p = 0.04$) and decreased number of transitions into the center ($t_{(26)} = 2.58$, $p = 0.01$) (Fig. 2b; Supplementary Fig. 3c). Light-dark box test showed a consistent tendency, featuring less time ($t_{(25)} = 2.81$, $p < 0.01$) and decreased frequency ($t_{(26)} = 4.12$, $p < 0.001$) to the light box (Fig. 2d). In summary, brain-specific *Stk24* cKO mice displayed a higher level of anxiety as compared to control WT mice.

No significant difference was detected in cognitive abilities and electrophysiological characteristics between WT and *Stk24* cKO mice

Given that the hippocampus plays a key role in learning and memory[10], we asked whether *Stk24* deletion influenced cognition since abnormal hippocampal formation was detected during development. A battery of behavioral tests was conducted, including Morris water maze, Y-maze, and novel object recognition, each of which tested for a specific set of cognitive abilities. The Morris water maze was widely used for measuring spatial learning and memory in rodents. No significant difference was detected in the learning curves between WT and cKO mice ($F_{(1,26)} = 0.70$, $p = 0.40$), showing similar spatial learning ability (Fig. 3a). Seven days after the last training trial, a memory test was carried out. The time in the target quadrant ($U = 80.00$, $p = 0.42$) and the number of transitions ($t_{(26)} = 0.93$, $p = 0.35$) were also equivalent between the groups, showing unaffected spatial memory in cKO mice (Fig. 3b). The Y-maze was used to test working memory. WT and *Stk24* cKO mice showed equivalency in the percentage of correct choices ($t_{(25)} = 0.24$, $p = 0.80$), indicating no difference in working memory (Fig. 3c). The novel object recognition test was used to assess recognition memory,

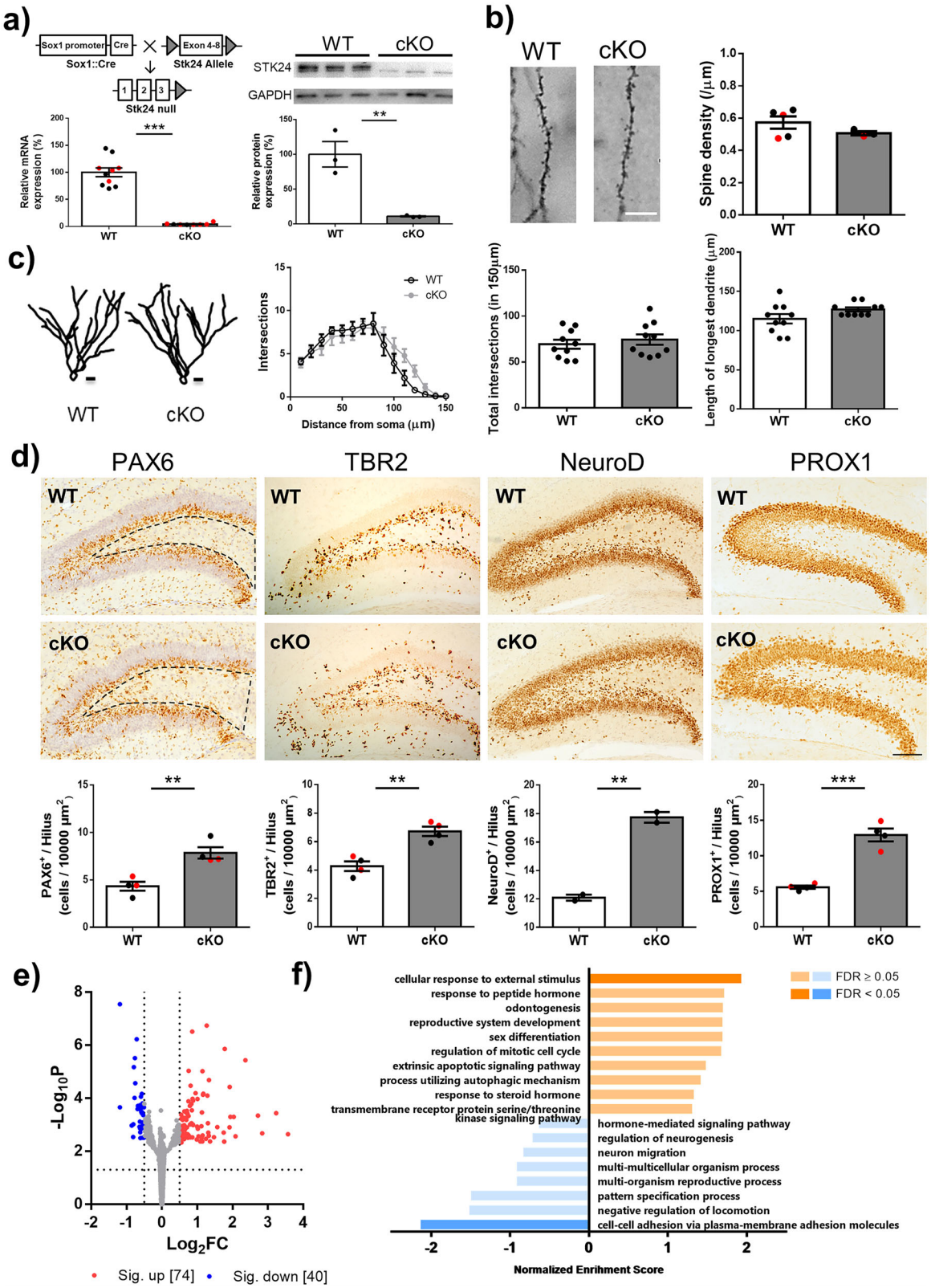

Fig. 1 | Brain-specific conditional knockout of *Stk24* caused disrupted postnatal hippocampal development. a *Stk24* cKO mice were obtained by crossing *Sox1::Cre* mice with *Stk24*$^{fl/}$ mice. *Stk24* expression was significantly decreased in cKO mice at the mRNA (left, $n = 8$–10) and protein (right, $n = 3$) levels. Black dots represent male mice, while red dots represent females. Unpaired t-test. **b** The spine densities were equivalent between the groups ($n = 3$–5). Black dots represent male mice, while red dots represent females. Unpaired t-test. Scale bar = 10 μm. **c** There was no significant difference in the intersections, total intersections, and the length of the longest dendrites ($n = 10$ neurons from each group). WT: 2 males, 3 females; cKO: 2 males, 1 female. Repeated two-way ANOVA and unpaired t-test. Scale bar = 10 μm. **d** *Stk24* cKO mice exhibited significantly more ectopic granule cells (PAX6, TBR2, PROX1: $n = 4$; NeuroD: $n = 2$). The enclosed regions represent ROI. Black dots represent male mice, while red dots represent females. Unpaired t-test. Scale bar = 100 μm. **e** Volcano plot of the DE genes with a p-value < 0.05 and a $|\log_2(\text{fold change})| > 0.5$ ($n = 3$). WT: 2 males, 1 female; cKO: 3 males. **f** Enriched BP pathways targeted by GO analysis. The data were presented as mean ± SEM for each group. $^*p < 0.05$, $^{**}p < 0.01$, $^{***}p < 0.001$.

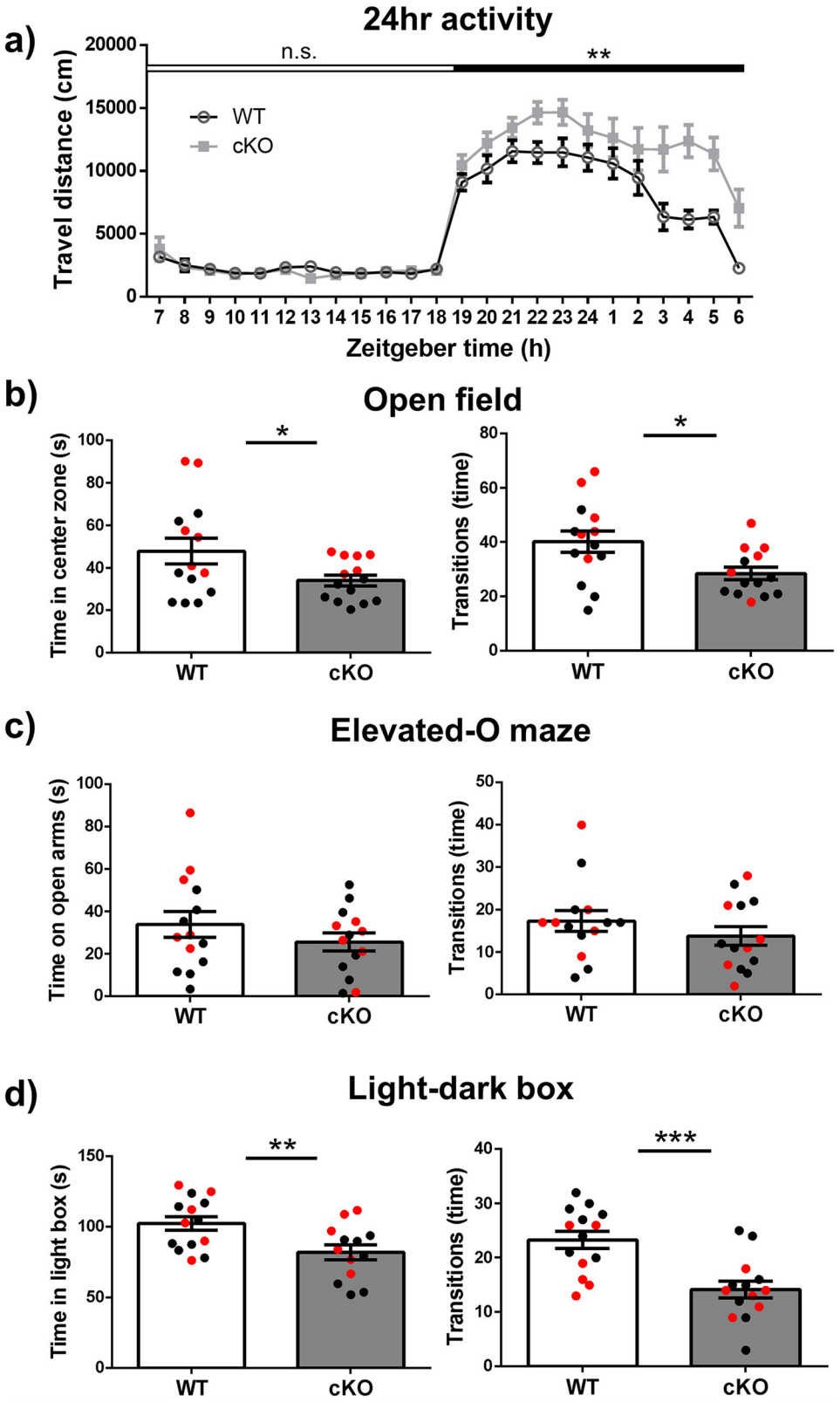

Fig. 2 | Brain-specific *Stk24* cKO mice exhibited hyperactivity and increased anxiety. a *Stk24* cKO exhibited longer travel distance during the active phase (ZT19-ZT6) as compared to WT mice ($n = 14$). WT: 8 males, 6 females; cKO: 8 males, 6 females. Repeated two-way ANOVA. **b** In the open field test, *Stk24* cKO mice spent longer time in the center zone and had higher frequency of entering the center area ($n = 14$). Black dots represent male mice, while red dots represent females. Unpaired t-test. **c** In the elevated O-maze, no significant difference was detected in the time mice spent on the open arms and the number of transitions ($n = 14$). Black dots represent male mice, while red dots represent females. Unpaired t-test. **d** In the light-dark box, *Stk24* cKO mice spent longer time in the light box and a greater number of transitions ($n = 14$). Black dots represent male mice, while red dots represent females. Unpaired t-test. The data were presented as mean ± SEM for each group. $^{*}p < 0.05$, $^{**}p < 0.01$, $^{***}p < 0.001$.

and the results were calculated as discrimination index (D.I.). Both WT and cKO group exhibited a D.I. of ~0.6, showing a tendency to novel objects; yet no difference was found in the recognition memory between the two groups ($t_{(26)} = 0.82$, $p = 0.41$) (Fig. 3d). Taken together, brain-specific *Stk24* deletion did not significantly affect the tested cognitive abilities.

Although *Stk24* cKO mice did not show impaired learning nor memory, we further examined the synaptic plasticity of hippocampal neurons, as these are believed to underpin cognitive functions. For this purpose, we investigated the electrophysiological characteristics of hippocampal neurons. Field excitatory postsynaptic potential (fEPSP) was recorded in the CA1 region of hippocampus to measure the long-term potentiation (LTP) and the paired-pulse facilitation (PPF). Our data revealed that WT and cKO mice displayed similar patterns of LTP ($F_{(1,12)} = 0.0001$, $p = 0.99$) and PPF ($F_{(1,18)} = 1.47$,

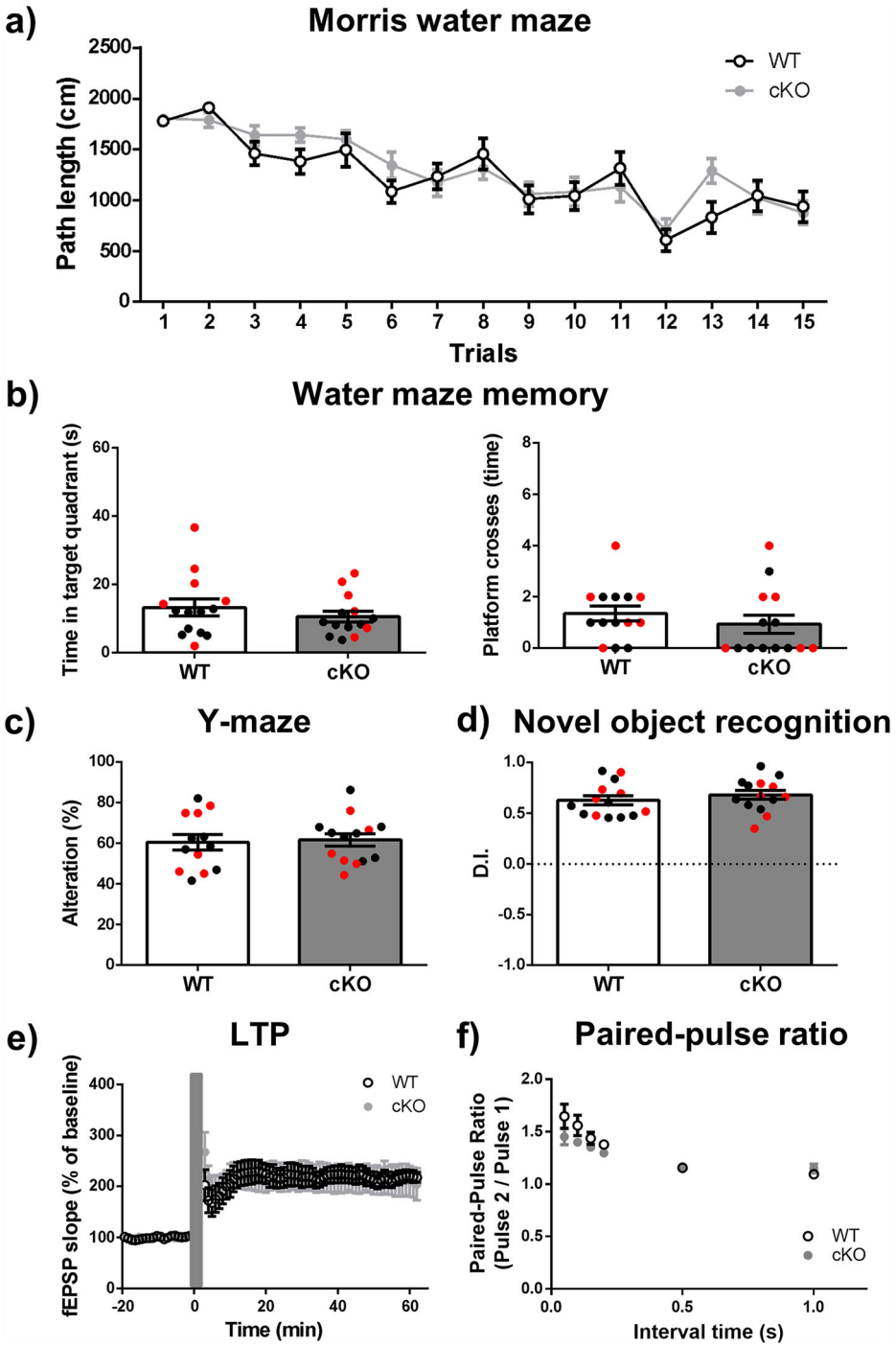

Fig. 3 | No significant difference was detected in cognitive abilities and electrophysiological characteristics between WT and *Stk24* cKO mice. a No significant difference was found in the learning curves between WT and *Stk24* cKO mice during Morris water maze test ($n = 14$). WT: 8 males, 6 females; cKO: 8 males, 6 females. Repeated two-way ANOVA. **b** In the memory test, WT and cKO mice exhibited equivalency in the time spent in target quadrant and the platform crosses ($n = 14$). Black dots represent male mice, while red dots represent females. Unpaired t-test. **c** WT and cKO mice showed comparable percentage of alterations in Y-maze ($n = 14$). Black dots represent male mice, while red dots represent females. Unpaired t-test. **d** In novel object recognition test, WT and cKO mice displayed similar percentage of D.I ($n = 14$). Black dots represent male mice, while red dots represent females. Unpaired t-test. **e** There was no significant difference in the pattern of LTP between the groups ($n = 7$ recording sites from 3 male mice for each group). Repeated two-way ANOVA. **f** There was no significant difference in the paired-pulse ratio between WT and *Stk24* cKO mice ($n = 10$ recording sites from 3 male mice for each group). Repeated two-way ANOVA. The data were presented as mean ± SEM for each group.

$p = 0.24$) (Fig. 3e, f), indicating unaffected neuronal plasticity in the absence of *Stk24*.

Brain-specific *Stk24* deletion decreased adult hippocampal neurogenesis

Stk24 cKO mice had showed disrupted hippocampal neurogenesis during brain development. Adding that emotional behavior has been proposed to share a link with adult hippocampal neurogenesis[11,12], although more research is needed, we were interested if *Stk24* altered adult hippocampal neurogenesis as well considering the increased anxiety and abnormal hippocampal development in *Stk24* cKO mice. To this end, mice were given 5-bromo-2'-deoxyuridine (BrdU) for two injections every other day (200 mg kg^{-1} per injection, i.p.) to label newly born cells. Twenty-eight days after the injections, mice were sacrificed and the brains were harvested for the assessment of adult hippocampal neurogenesis. Several neurogenesis markers were selected for IHC staining including KI67, TBR2, NeuroD, and DCX. Brain-specific *Stk24* cKO mice were found to have decreased numbers of $Ki67^+$ ($t_{(16)} = 1.81$, $p = 0.08$), TBR2 ($U = 10.00$, $p < 0.01$), $NeuroD^+$ ($U = 0.00$, $p < 0.01$), and DCX^+ ($t_{(16)} = 3.19$, $p < 0.01$) cells in the dentate gyrus of the hippocampus, where the neurogenesis occurs, indicating impaired adult hippocampal neurogenesis (Fig. 4a). To further confirm whether cKO mice had fewer newly born neurons, we double-labeled the NeuN and BrdU by immunofluorescent (IF) staining, and a significant reduction of co-localized $NeuN^+/BrdU^+$ cells was observed in *Stk24* cKO mice ($t_{(18)} = 3.29$, $p < 0.01$) (Fig. 4b), confirming the decreased adult hippocampal neurogenesis.

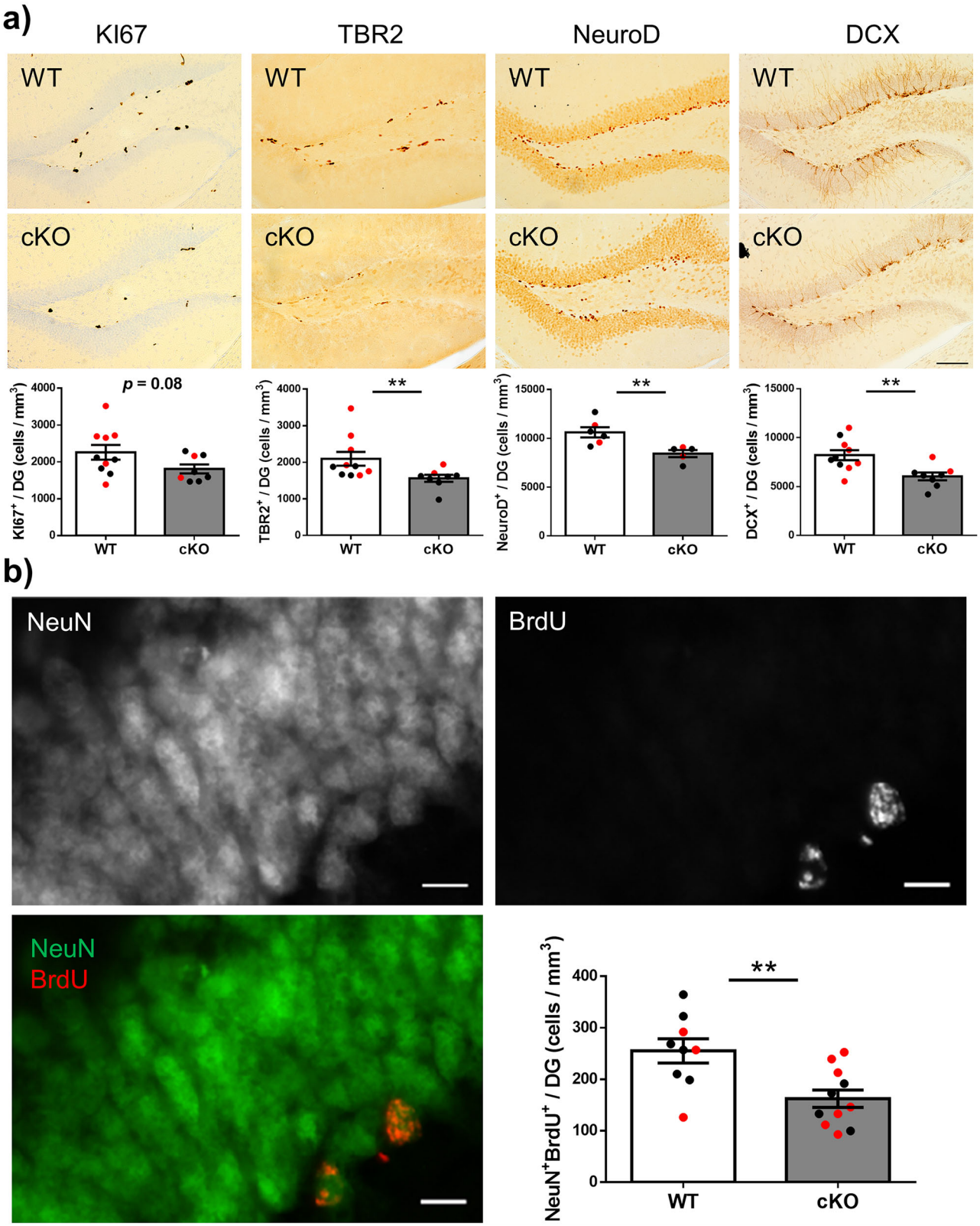

Fig. 4 | Brain-specific *Stk24* deletion decreased adult hippocampal neurogenesis. **a** Significant decreases were found in the number of $TBR2^+$ ($n = 8–10$), $NeuroD^+$ ($n = 5–6$), and DCX^+ ($n = 8–10$) cells in the dentate gyrus of *Stk24* cKO mice as compared to WT, while no difference was found in the number of $KI67^+$ cells ($n = 8–10$). Black dots represent male mice, while red dots represent females. Unpaired t-test for KI67, TBR2, and DCX. Mann–Whitney U test for NeuroD. Scale bar = 100 μm. **b** *Stk24* cKO mice exhibited a significantly lower level of colocalized $NeuN^+/BrdU^+$ cells than control WT ($n = 9–11$). Black dots represent male mice, while red dots represent females. Unpaired t-test. Scale bar = 10 μm. The data were presented as mean ± SEM for each group. $^*p < 0.05$, $^{**}p < 0.01$, $^{***}p < 0.001$.

Brain-specific *Stk24* deletion altered HPA reactivity but not the downstream GR signaling pathway

Dysregulated plasma cortisol and altered stress response are important features of anxiety disorders[13]. Since *Stk24* cKO mice exhibited increased anxiety-like behavior, we further investigated the hypothalamus-pituitary-adrenal (HPA) axis reactivity to see whether the regulation of corticosterone had been altered. As the two most major stress hormones, corticosterone and cortisol are considered as indicators for stress response and are regulated by the HPA axis, with the former being the main stress hormone in rodents and the latter being predominant in humans[14,15]. In fact, plasma corticosterone is one of the major factors to influence adult hippocampal neurogenesis and anxiety[16,17]. We measured the plasma corticosterone levels at three different time points: under basal condition, after 30 min of restraint stress, and after 60 min of recovery from restraint stress. Our results showed significantly higher corticosterone levels in *Stk24* cKO mice under the stressed condition as compared to control WT ($t_{(16)} = 4.61$, $p < 0.001$). However, there was no significant difference under basal ($t_{(16)} = 0.40$, $p = 0.69$) nor recovered ($t_{(16)} = 0.23$, $p = 0.81$) conditions between the groups (Fig. 5a). Moreover, we also assessed the hippocampal neuronal activation under basal and stressed conditions, respectively, since the hippocampus was the upstream of HPA axis and could mediate the HPA axis reactivity[18,19]. We performed IHC staining for the detection of c-FOS, an immediate early gene known as the molecular marker of neural activity, in the hippocampus[20]. Consistent with the corticosterone levels, IHC staining showed an increased number of c-FOS$^+$ cells in *Stk24* cKO mice under stressed condition ($U = 7.00$, $p = 0.02$), while equivalent numbers were measured between WT and cKO groups under the basal condition ($U = 16.50$, $p = 0.55$) (Fig. 5b, c). In summary, brain-specific *Stk24* deletion caused increased neural activity in the hippocampus under stressed conditions, along with a higher plasma corticosterone level. Yet no significant difference was found under basal nor recovered states at the time points measured.

In our data, *Stk24* exerted a remarkable influence on anxiety and HPA reactivity. To further understand the possible mechanism at the molecular level, we investigated the glucocorticoid receptor (GR) signaling pathway in the hippocampus. Although the GR signaling is famous for its connection with the HPA axis reactivity in the paraventricular nucleus (PVN) of the hypothalamus, the GR signaling in the hippocampus is more likely associated with anxiety and stress, and it is also where the highest levels of glucocorticoid binding occured[21–24]. Hippocampal tissues were collected from basal group and stress group. Real-time PCR was then performed to quantify the mRNA expression levels of GR signaling pathway-related genes including *Crh* and *Crhr1*, which were demonstrated to play important roles in emotional responses, and the GR downstream genes GR (*Nr3c1*), *Sgk1, Fkbp5*, and *Gilz*[25,26] (Fig. 5d). As the *Stk24* expression was confirmed deleted (basal: $U = 0.00$, $p < 0.001$; stress: $U = 0.00$, $p < 0.001$), a great increase in the *Crh*, but not *Crhr1*, expression was detected in *Stk24* cKO mice in both basal and stress groups (basal *Crh*: $U = 2.00$, $p < 0.01$; basal *Crhr1*: $U = 12.00$, $p = 0.14$; stress *Crh*: $U = 0.00$, $p < 0.001$; stress *Crhr1*: $U = 20.00$, $p = 0.63$). Nevertheless, no significant difference was found in most of the GR signaling-related genes (basal GR: $U = 24.00$, $p > 0.99$; basal *Fkbp5*: $U = 14.00$, $p = 0.22$; basal *Gilz*: $U = 22.00$, $p = 0.83$; stress GR: $U = 18.00$, $p = 0.47$; stress *Fkbp5*: $U = 11.00$, $p = 0.10$; stress *Gilz*: $U = 15.00$, $p = 0.27$), except for Sgk1 (basal: $U = 5.00$, $p = 0.01$; stress: $U = 14.00$, $p = 0.22$). These results suggested an alteration in the *Crh* and *Sgk1* signaling caused by the *Stk24* deletion. Put together, *Stk24* altered the neural activity in the hippocampus under stressed conditions and may consequently mediated the HPA axis reactivity and the downstream gene expressions.

Discussion

In this study, we set out to investigate the roles of *Stk24* in the hippocampus by testing brain development, adult hippocampal neurogenesis, animal behavior, and stress response. Brain-specific *Stk24* cKO mice were used in this research. When examining the neuronal morphology and postnatal neurogenesis, ectopic neurons were found in *Stk24* cKO mice during postnatal brain development, while the neuronal morphology including dendritic spine density, dendrite branching, and dendrite length, remained unaffected. The decreased adult hippocampal neurogenesis was also detected during their adulthood, and these phenotypes were in consistent with the RNA-sequencing findings, where neurogenesis, neuronal migration, and pattern specification were indicated as the down-regulated pathways in *Stk24* cKO mice. As for animal behavior, *Stk24* cKO mice exhibited increase anxiety, but not impaired cognitive abilities. When we further looked into the possible mechanisms behind the increased anxiety, a higher level of stress-induced plasma corticosterone was measured, indicating altered HPA axis reactivity. The neural activity in the hippocampus, which is known to mediate the HPA axis, was also shown to be elevated after acute stress. Meanwhile, altered expressions of the GR signaling-related genes, *Crh* and *Sgk1*, were found in the hippocampus of cKO mice. In conclusion, brain-specific *Stk24* deletion disrupted the hippocampal formation during brain development and adult hippocampal neurogenesis. The absence of *Stk24* also increased anxiety-like behavior and altered the stress response including neural activity, HPA axis reactivity, and GR signaling-related gene expressions.

It has become increasingly evident that *Stk24* plays an essential role in neuronal development. Several previous studies have demonstrated that *Stk24* is important for cortical neuronal migration and hippocampal neuronal filopodia. It is also reported to regulate axonal regeneration in both central nervous system and peripheral nervous systems by shRNA[5–7]. In our study, *Stk24* cKO mice featured ectopic granule cells in the dentate gyrus during hippocampal formation. Intriguingly, unlike previous result[5], we failed to detect a significant reduction in the spine density in cKO mice. No significant difference was detected in neuronal morphology by Sholl analysis either. While many confounding factors may lead to such inconsistency, the biggest difference is that we used "gene knockout mice" instead of "shRNA-mediated knockdown". Moreover, for adult hippocampal neurogenesis, there was no evident histological changes between adult WT and *Stk24* cKO mice, unlike what we had observed during brain development. Other factors might be involved and probably compensate for the effects of *Stk24* deletion after brain development. Despite normal hippocampal anatomy, decreased level of adult hippocampal neurogenesis was found, including reduced number of KI67$^+$, TBR2$^+$, NeuroD$^+$, DCX$^+$, and NeuN$^+$/BrdU$^+$ cells. This suggested that the reduced number of proliferating cells may be the cause of neurogenesis deficit in *Stk24* cKO mice. Past studies have suggested a connection between hippocampal neurogenesis and cognitive functions and/or anxiety[12,27]; yet some suggested otherwise[28]. In our results, brain-specific *Stk24* cKO mice were found to exhibit anxiety-like behavior, while the cognitive abilities and the electrophysiological characteristics were not significantly affected. Since we deleted *Stk24* in the whole brain, it is unclear whether the behavioral phenotypes were resulted from the altered hippocampal neurogenesis caused by *Stk24* deletion. We could not rule out the possibility that other brain regions such as cortex or amygdala may also play a role in it. Further investigation is needed to address this.

Although the link between anxiety-like behavior and altered adult hippocampal neurogenesis remains unclear, we examined other mechanisms known to be related. To this end, we measured the stress response, from the HPA axis reactivity to the molecular changes of GR signaling. Under basal conditions, mice with *Stk24* deletion exhibited an upregulation of *Crh* and a downregulation of *Sgk1* in the hippocampus. A past study has indicated that mice with corticotropin-releasing hormone (CRH) overproduction displayed anxiogenic behavior[29]. The elevated *Crh* expression in *Stk24* cKO mice might explain the anxiety-like behavior; however more evidence is required. *Sgk1* is a serine/threonine kinase, which has been shown to play a role in neurogenesis, memory, neuronal plasticity and dendritic growth[30–33]. The activity of SGK1 is down-regulated in post-mortem brains in post-traumatic stress disorder, and inhibition of SGK1 results in anhedonic–like behavior in rats[34], suggesting a role of *Sgk1* in emotional response. In our result, we detected lower levels of hippocampal *Sgk1* expression in cKO mice. While no significant impairment was observed in the cognitive abilities and neuronal plasticity, it remained

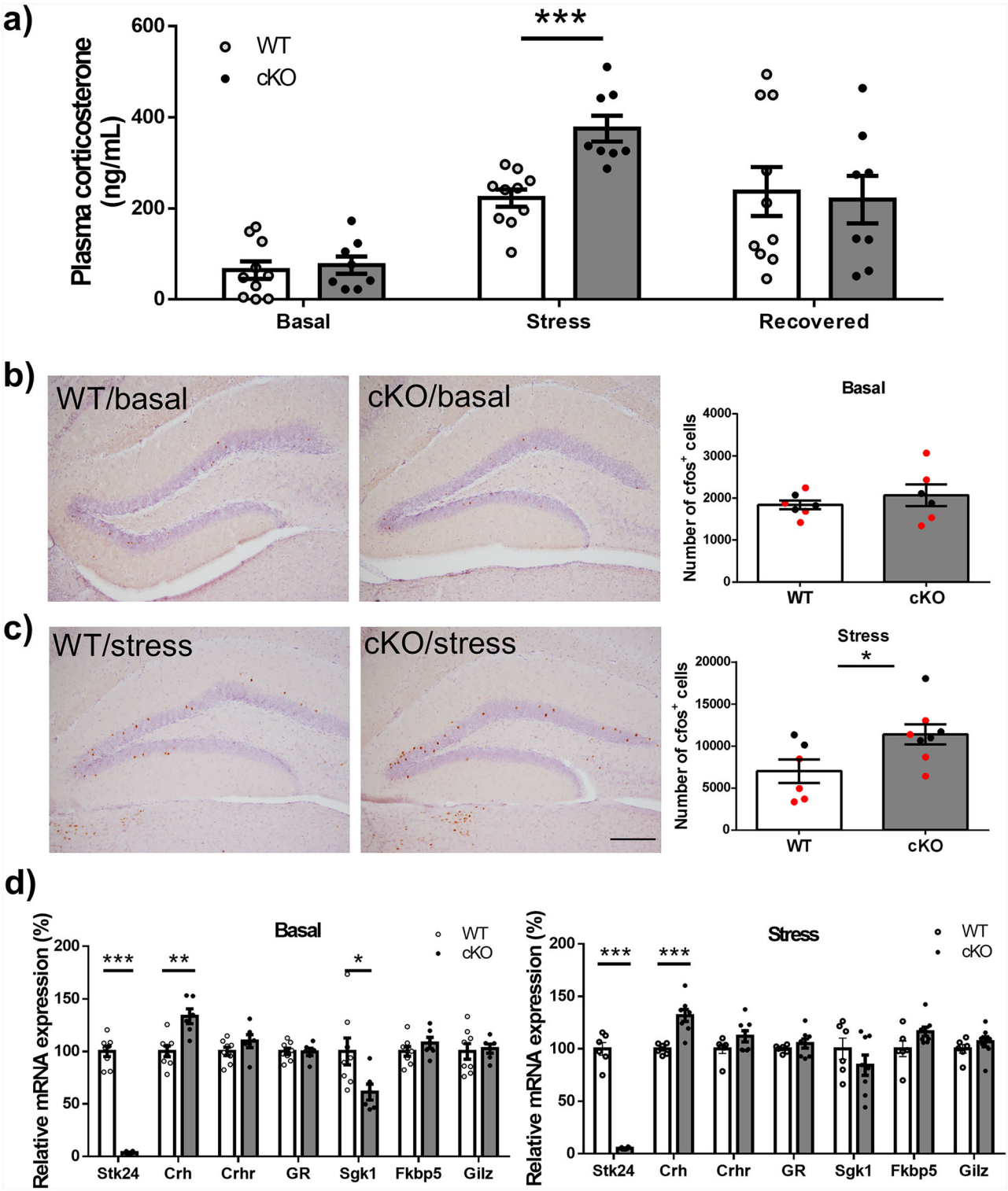

Fig. 5 | Brain-specific *Stk24* deletion altered HPA reactivity but not the downstream GR signaling pathway. a *Stk24* cKO mice had a significantly higher level of plasma corticosterone under stress, while there was no significant difference between WT and cKO mice under the basal and recovered conditions ($n = 8–10$). WT: 4 males, 6 females; cKO: 6 males, 2 females. Unpaired t-test for each condition. **b** The c-FOS expressions were comparable between WT and *Stk24* cKO mice under basal condition ($n = 6–7$). Black dots represent male mice, while red dots represent females. Mann–Whitney U test. Scale bar = 100 μm. **c** *Stk24* cKO mice displayed increased number of c-FOS$^+$ cells under stress as compared to WT ($n = 6–8$). Black dots represent male mice, while red dots represent females. Mann–Whitney U test. Scale bar = 100 μm. **d** Either under basal condition ($n = 6–8$) or stressed condition ($n = 6–8$), *Stk24* was confirmed deleted in cKO mice; *Crh* was found upregulated in cKO mice in both basal and stressed states, while most of the other gene expressions were equivalent between WT and cKO mice, except for *Sgk1*. Basal WT: 4 males, 4 females; Basal cKO: 2 males, 4 females; Stress WT: 2 males, 4 females; Stress cKO: 4 males, 4 females. Mann–Whitney U test for each gene. The data were presented as mean ± SEM for each group. $^*p < 0.05$, $^{**}p < 0.01$, $^{***}p < 0.001$.

unclear whether the decreased *Sgk1* level was involved in anxiety-like behavior. The role of *Sgk1* in Stk24 deleted mice remains to be answered. Furthermore, when exposed to acute stress, *Stk24* cKO mice displayed significantly increased *Crh* expression and increased neural activity in the hippocampus. Consistently, the stress-induced corticosterone was higher in cKO mice as compared to WT, while no significant differences were detected in the downstream regulation of GR. Based on current data, *Stk24* influences the expression of *Crh* under basal and stress conditions, and the deletion of *Stk24* could disrupt the stress response. However, the specific mechanism remains undetermined.

In conclusion, several previous studies have demonstrated the importance of *Stk24* in neuronal development, migration, and regeneration. Herein, we used brain-specific *Stk24* cKO mice to provide evidence that *Stk24* played a role in modulating anxiety, hippocampal neurogenesis, and stress response including HPA axis reactivity, *Crh* expression, and *Sgk1* expression. Further understanding of the underlying cellular mechanisms of *Stk24* is needed to interrogate how the brain *Stk24* plays its role.

Materials and methods

Animals

Stk24 conditional knockout mice were obtained by crossing *Stk24* floxed mice (National Laboratory Animal Center, Taiwan) with *Sox1::Cre* mice (Access No. CDB0525K)[8]. Mice were housed in individually ventilated cages (IVC) in the AAALAC certified animal facility, where they were maintained in a 12:12 h light-dark cycle at a temperature of 22 °C and a humidity level of 60–70%. Animals had *ad libitum* access to food and water. We have complied with all relevant ethical regulations for animal use. All procedures were carried out in accordance with the local regulations and approved by the Institutional Animal Care and Use Committee at Chang Gung University (Permit Number: CGU112-116). All following experimental details were previously described[35,36]. The sex of mice for each experiment were indicated in different colors in the figure, or were described in the figure captions.

mRNA quantification

Hippocampi were isolated and homogenized in TRIzol™ reagent (Invitrogen, 15596026, CA, USA), followed by Phenol-Chloroform extraction of total RNA. cDNA was then synthesized using Modified MMLV Reverse Transcriptase (Protech, Taipei, Taiwan). Gene expression levels were calculated with the ΔΔCt method and normalized against a Gapdh control. Experiments were performed in duplicate.

The table below shows the primer sequences used for real-time PCR.

	Forward	Reverse
Stk24	CAGCTGACGGATACCCAGAT	CAGTGTGGGAGGGTTGTTCT
Crh	AGCCCTTGAATTTCTTGCAG	AGCCCTTGAATTTCTTGCAG
Crhr1	AGCCCTTGAATTTCTTGCAG	CTGCCATCCGGAAGAGGT
GR	AGGCGATACCAGGATTCAGA	GCAAAGCATAGCAGGTTTCC
Sgk1	CTGCTCGAAGCACCCTTACC	TCCTGAGGATGGGACATTTTCA
Fkbp5	AACGGAAAGGCGAGGGATAC	ACACCACATCTCGGCAATCA
Gilz	AACACCGAAATGTATCAGACCC	GTTTAACGGAAACCAAATCCCCT
Gapdh	TGCACCACCAACTGCTTAGC	GGCATGGACTGTGGTCATGAG

Western blot

Hippocampi were isolated and homogenized in 1% SDS solution at 100 °C for 5 min, followed by the quantification of protein extracts using a Bradford protein assay. Equal amounts of protein samples were separated by 10% SDS–polyacrylamide gel electrophoresis and were transferred to a polyvinylidene difluoride (PVDF) membrane (Millipore, Cork, Ireland). Membranes were incubated with 5% non-fat milk for 1 h at room temperature and then with diluted primary antibodies (STK24, A10576, ABclonal, MA, USA; GAPDH, sc-32233, Santa Cruz, TX, USA) in 5% non-fat milk at 4 °C overnight. After being washed with TBST, membranes were incubated with diluted horseradish peroxidase (HRP)-conjugated secondary antibody (goat anti-rabbit IgG, bs-0295G-HRP, Bioss, MA, USA; goat anti-mouse IgG, bs-0296G-HRP, Bioss, MA, USA) for 1 h at room temperature. Blots were visualized using Immobilon Western Chemiluminescent HRP Substrate (WBKLS0500, Millipore, MA, USA) and were detected with a ChemiDoc XRS+ imaging system (Bio-Rad). The protein signals were quantified and normalized against GAPDH control using Image-J software.

Golgi staining

Brains were harvested from postnatal day 13 (P13) mice and were impregnated with Golgi-Cox solution for 7 days, followed by 2 days of dehydration in sucrose. Brain sections at a thickness of 150 μm were collected using a microtome and were then stained using a superGolgi Kit (003010, Bioenno Tech, CA, USA) in accordance with the manufacturer's instructions. For the quantification of spine density, we selected 36 dendrites per animal from the granule cells in the dentate gyrus of the hippocampus and calculated the number of dendritic spines. Spine density was then measured as the number of dendritic spines divided by the length of chosen dendrites. Sholl analysis was performed using the Neurolucida software (MicroBrightField Bioscience, Williston, VT, USA).

Immunohistochemistry, immunofluorescence, and quantification

Brains were harvested and fixed in 4% paraformaldehyde overnight, followed by dehydration in 25% sucrose at 4 °C. Brain cryosections at a thickness of 40 μm were collected and stored in 60% glycerol before staining.

For immunohistochemical staining, brain sections were mounted on SuperFrost Plus slides (Thermo, PA, USA) and air-dried overnight. The slides were incubated with 0.01 M citric acid buffer (pH = 6.4) for 20 min at 95 °C (40 min in the case of KI67), 3% H_2O_2 for 5 min, and then diluted primary antibody (PAX6, AB2237, Millipore Sigma, MO, USA; TBR2, ab23345, Abcam, Cambridge, UK; PROX1, AB5475, Millipore Sigma, MO, USA; NeuroD, sc-1084, Santa Cruz, TX, USA; KI67, ab16667, Abcam, Cambridge, UK; DCX, ab18723, Abcam, Cambridge, UK; c-FOS: sc-8047, Santa Cruz, TX, USA) at room temperature overnight. Slides were rinsed with PBS for 15 min (3 times) between each step. Subsequently, a standard IgG ABC kit (PK-6101, Vector Labs, CA, USA) was used according to the manufacturer's instructions, and the slides were incubated with 3,3'-Diaminobenzidine (DAB) tablets (D4293-50SET, Millipore Sigma, MO, USA). Sections were then counterstained with hematoxylin and mounted with a DPX mountant (06522, Millipore Sigma, Madrid, Spain). Experimental details were described previously[37].

For the immunofluorescent staining for NeuN/BrdU double labeling, brain sections were incubated with 2 N HCl for 15 min at 37 °C, neutralized with boric acid (pH = 8.5) for 5 min at room temperature, and washed with PBS for 15 min before the incubation with diluted primary antibody (NeuN, MAB377, Millipore Sigma, MO, USA; BrdU, ab6326, Abcam, Cambridge, UK) for 8 hr at room temperature. After being rinsed with PBS for 15 min, brain sections were incubated with the diluted fluorescent secondary antibody (Alexa Fluor 488: A21121, Invitrogen, OR, USA; Texas Red: A11007, Invitrogen, OR, USA) for 2 h at room temperature. Sections were then washed with PBS for 15 min and mounted on SuperFrost Plus slides (Thermo, PA, USA), air-dried for 20 min, and mounted with Fluoromount-G (100-20, SouthernBiotech, AL, USA).

For quantification, all sections were examined under a microscope with a magnification of 200x. Antibody-stained cells were counted in the bilateral dentate gyrus of the hippocampus every eight sections through the entire extent of the granule cell layer (six sections per mouse). The number of cell counts was then multiplied by eight to obtain an estimate of total antibody-stained cells in the region of interest (ROI). The ROI area was measured using ImageJ and then multiplied by the brain slice thickness to estimate its volume. Data represented as the number of antibody-stained cells normalized against the ROI volume.

RNA-sequencing

Library preparation and sequencing. Purified RNA was used to prepare sequencing libraries using the TruSeq Stranded mRNA Library Prep Kit (Illumina) following the manufacturer's instructions. Briefly, mRNA was purified from 1 μg of total RNA using oligo(dT)-coupled magnetic beads and fragmented at elevated temperatures. First-strand cDNA was synthesized with reverse transcriptase and random primers, followed by second-strand cDNA synthesis to generate double-stranded cDNA. The cDNA fragments were adenylated at their 3' ends, and adaptors were ligated. The library products were enriched via PCR and purified using the AMPure XP system (Beckman Coulter). The libraries were validated with the Qsep400 System (Bioptic Inc.) and quantified using a Qubit 2.0 Fluorometer (Thermo Scientific). Sequencing was performed on the Illumina NovaSeq X Plus platform with 150 bp paired-end reads generated by Genomics, BioSci & Tech Co., Taiwan.

Behavioral testing

Behavioral tests were carried out on mice at the age of 8–12 weeks and were conducted during the mouse active phase. Mice were randomized between WT and cKO to minimize the current environmental effects. The experimental details were described below.

Grip. The grip strength meter (47200, UGO BASILE, VA, Italy) consisted of a grasping bar which was fitted to a forced transducer connected to the peak amplifier. Mice were allowed to grip the grasping bar while their tails were held and slightly pulled by the experimenters. The maximal grip force was recorded. Each mouse was tested three times and the average grip force was recorded.

Rotarod. Mice were placed on the rotarod apparatus (UGO BASILE, VA, Italy) and the latency for them to fall off the rod was recorded manually. The rod rotated at an initial speed of 4 rpm and an accelerated speed of 9 rpm per minute. Each mouse was tested three times and the average falling latency was recorded.

Locomotor activity. Mice were individually placed in the cage and had *ad libitum* access to food and water. The animals were maintained in the behavioral room in a 12:12 light-dark cycle under 24 h continuous recording. The total travel distance was measured using Ethovision software.

Open field. Mice were allowed to explore in a circular-shaped area (radius = 60 cm) for 5 min with a lamp illuminating the center. The total distance, the time spent in the center area (radius = 40 cm), and the frequency of entering the center area were recorded by Ethovision software.

Elevated O-maze. The O-shaped maze (radius = 55 cm) was elevated 60 cm above the floor and consisted of the open arms and the closed arms. The closed arms featured 15 cm-high walls. Mice were placed in the closed arm and allowed to freely move for 5 min. The total distance, the time spent in the open arms, and the frequency of entering open arms were measured by Ethovision software.

Light-dark box. The light-dark box was divided into a covered dark chamber and a coverless light chamber. Mice were put into the covered dark chamber and allowed to freely move between the two chambers via a door for 5 min. The time spent in the light chamber and the frequency of transitions were recorded by Ethovision software.

Morris water maze. A circular water tank (radius = 130 cm) was filled with 22 °C water, and a circular platform (radius = 10 cm) was located inside the tank, submerged 1.5 cm below the water surface. The water had been colored with white acrylic turpentine to cover the platform. Mice were put into the tank at three different starting positions, which refer to the three quadrants other than the quadrant with the platform. Each mouse was trained to search for the hidden platform and stayed on it for 30 s, three trials a day for five consecutive days. The time each mouse used to find the platform was recorded using Ethovision software. Seven days after the last training, a one-minute memory test was performed with the platform removed. The time each mouse spent in the target zone (quadrant where the platform was previously) was recorded by Ethovision software.

Y-maze. Mice were placed in a Y-shaped maze and were allowed to freely move for 5 min. An alteration was defined as consecutive entries into three different arms without any repeats, while the max alteration indicated the maximal possible alterations according to the number of total entries, both of which were analyzed using Ethovision software. The percentage of alteration (%) was calculated as the number of alterations divided by max alteration.

Novel object recognition. Mice were allowed to freely move in the empty chamber (30 × 30 × 25 cm) for 10 min on day 1. Then on day 2, mice were exposed to two identical objects in the chamber and were also allowed to freely explore for 10 min. On day 3, one of the objects was replaced with a novel one. Mice were allowed to explore for 10 min. The time mice spent to explore the objects were measured using Ethovision software, and the discrimination index (D.I.) was calculated according to the below formula.

$$D.I. = \frac{(Time\ exploring\ novel\ object - Time\ exploring\ familiar\ object)}{(Time\ exploring\ novel\ object + Time\ exploring\ familiar\ object)} \times 100\%$$

For the objects used in the test, the two identical ones were white plastic cylinders, with a diameter of 4 cm and a height of 6 cm. The novel object introduced on day 3 was a yellow, dumbbell-shaped plastic piece with equilateral triangles attached to each end, each triangle having a side length of 4.5 cm and the total height of the object was 5.2 cm.

Electrophysiology

A bipolar stainless steel stimulating electrode (Frederick Haer Company, ME, USA) (10 Meg-ohm impedance) and a glass pipette filled with 3 M NaCl were positioned in CA1. For LTP experiments, field excitatory postsynaptic potential (fEPSP) was evoked every 20 s for the first 20 min as baseline, and then a high-frequency stimulation (HFS) which composed of five trains of 100 pulses at 100 Hz with an inter-train interval of 20 s was introduced to trigger LTP. fEPSP activity was subsequently recorded for 1 h to assess LTP. For paired pulse, it was determined for five inter-pulse intervals (50, 100, 150, 200, 500, 1000 milliseconds). Paired of pulses were repeated four times for each inter-pulse interval, and the paired pulse ratio was calculated as the second response divided by the first response. Electrophysiological traces were amplified with an amplifier (Multiclamp 700B: Axon Instruments, CA, USA). All signals were low-pass–filtered at 1 kHz and digitized at 10 kHz using a CED Micro 1401 mKII interface (Cambridge Electronic Design, Cambridge, UK). Data were collected using Signal software (Cambridge Electronic Design, Cambridge, UK). Synaptic responses were normalized to the average of the baseline.

Corticosterone assay

Blood samples were collected by facial vein puncture at three different time points: under baseline (basal) conditions, after 30 min of restraint stress, and after 60 min of recovery from restraint stress. Plasma was separated from whole blood by centrifugation (3000 rpm, 4 °C, 15 min) and stored at −80 °C until used. Plasma corticosterone concentration was measured using the Corticosterone ELISA kit (ADI-900-097, Enzo Life Sciences, NY, USA) according to the manufacturer's instructions.

Statistics and reproducibility

The data were presented as mean ± SEM for each group. $^{*}p < 0.05$, $^{**}p < 0.01$, $^{***}p < 0.001$. Statistical analysis was performed using Graphpad Prism 6.0 software. All data were tested for normal distribution using D'Agostino and Pearson omnibus normality test (Supplementary Table 1) and were further analyzed via unpaired t-test, Mann–Whitney U test, or an analysis of variance (ANOVA) as appropriate. The sample size and the number of replications were determined by referencing previous studies in the same field. All experiments were replicated at least once or replicated on more than one cohort of mice. Replication attempts were successful and the observed results were consistent.

Reporting summary

Further information on research design is available in the Nature Portfolio Reporting Summary linked to this article.

Data availability

The RNA sequencing data have been deposited at the NCBI Sequence Read Archive (SRA) (accession number PRJNA1242514). Source data were available in Supplementary Data, and the uncropped blots were provided in Supplementary Information (Supplementary Fig. 4).

Received: 15 March 2024; Accepted: 2 April 2025;
Published online: 25 April 2025

References

1. Dan, I., Watanabe, N. M. & Kusumi, A. The Ste20 group kinases as regulators of MAP kinase cascades. *Trends Cell Biol.* **11**, 220–230 (2001).
2. Zhou, T. H. et al. Identification of a human brain-specific isoform of mammalian STE20-like kinase 3 that is regulated by cAMP-dependent protein kinase. *J. Biol. Chem.* **275**, 2513–2519 (2000).
3. Lu, T.-J. et al. Inhibition of cell migration by autophosphorylated mammalian sterile 20-like kinase 3 (MST3) involves paxillin and protein-tyrosine phosphatase-PEST. *J. Biol. Chem.* **281**, 38405–38417 (2006).
4. Irwin, N., Li, Y. M., O'Toole, J. E. & Benowitz, L. I. Mst3b, a purine-sensitive Ste20-like protein kinase, regulates axon outgrowth. *Proc. Natl Acad. Sci. USA* **103**, 18320–18325 (2006).
5. Ultanir, S. K. et al. MST3 kinase phosphorylates TAO1/2 to enable Myosin Va function in promoting spine synapse development. *Neuron* **84**, 968–982 (2014).
6. Tang, J. et al. Cdk5-dependent Mst3 phosphorylation and activity regulate neuronal migration through RhoA inhibition. *J. Neurosci.* **34**, 7425–7436 (2014).
7. Lorber, B., Howe, M. L., Benowitz, L. I. & Irwin, N. Mst3b, an Ste20-like kinase, regulates axon regeneration in mature CNS and PNS pathways. *Nat. Neurosci.* **12**, 1407–1414 (2009).
8. Takashima, Y. et al. Neuroepithelial cells supply an initial transient wave of MSC differentiation. *Cell* **129**, 1377–1388 (2007).
9. Huang, G. J. et al. Ectopic cerebellar cell migration causes maldevelopment of Purkinje cells and abnormal motor behaviour in Cxcr4 null mice. *PLoS One* **9**, e86471 (2014).
10. Bannerman, D. M. et al. Double dissociation of function within the hippocampus: spatial memory and hyponeophagia. *Behav. Neurosci.* **116**, 884–901 (2002).
11. Hill, A. S., Sahay, A. & Hen, R. Increasing Adult Hippocampal Neurogenesis is Sufficient to Reduce Anxiety and Depression-Like Behaviors. *Neuropsychopharmacology* **40**, 2368–2378 (2015).
12. Revest, J. M. et al. Adult hippocampal neurogenesis is involved in anxiety-related behaviors. *Mol. Psychiatry* **14**, 959–967 (2009).
13. Strohle, A. & Holsboer, F. Stress responsive neurohormones in depression and anxiety. *Pharmacopsychiatry* **36**, S207–214 (2003).
14. Joëls, M., Karst, H. & Sarabdjitsingh, R. A. The stressed brain of humans and rodents. *Acta Physiologica* **223**, e13066 (2018).
15. Vale, W., Spiess, J., Rivier, C. & Rivier, J. Characterization of a 41-residue ovine hypothalamic peptide that stimulates secretion of corticotropin and β-endorphin. *Science* **213**, 1394–1397 (1981).
16. Cameron, H. A. & Gould, E. Adult neurogenesis is regulated by adrenal steroids in the dentate gyrus. *Neuroscience* **61**, 203–209 (1994).
17. Mitra, R. & Sapolsky, R. M. Acute corticosterone treatment is sufficient to induce anxiety and amygdaloid dendritic hypertrophy. *Proc. Natl Acad. Sci. USA* **105**, 5573–5578 (2008).
18. Cole, A. B., Montgomery, K., Bale, T. L. & Thompson, S. M. What the hippocampus tells the HPA axis: Hippocampal output attenuates acute stress responses via disynaptic inhibition of CRF+ PVN neurons. *Neurobiol. Stress* **20**, 100473 (2022).
19. Herman, J. P. & Cullinan, W. E. Neurocircuitry of stress: central control of the hypothalamo–pituitary–adrenocortical axis. *Trends Neurosci.* **20**, 78–84 (1997).
20. Bullitt, E. Expression of c-fos-like protein as a marker for neuronal activity following noxious stimulation in the rat. *J. Comp. Neurol.* **296**, 517–530 (1990).
21. Claes, S. Corticotropin-releasing hormone (CRH) in psychiatry: from stress to psychopathology. *Ann. Med.* **36**, 50–61 (2004).
22. Maras, P. M. & Baram, T. Z. Sculpting the hippocampus from within: stress, spines, and CRH. *Trends Neurosci.* **35**, 315–324 (2012).
23. Aronsson, M. et al. Localization of glucocorticoid receptor mRNA in the male rat brain by in situ hybridization. *Proc. Natl Acad. Sci. USA* **85**, 9331–9335 (1988).
24. Reul, J. M. & de Kloet, E. R. Two receptor systems for corticosterone in rat brain: microdistribution and differential occupation. *Endocrinology* **117**, 2505–2511 (1985).
25. Timpl, P. et al. Impaired stress response and reduced anxiety in mice lacking a functional corticotropin-releasing hormone receptor 1. *Nat. Genet* **19**, 162–166 (1998).
26. Muller, M. B. et al. Limbic corticotropin-releasing hormone receptor 1 mediates anxiety-related behavior and hormonal adaptation to stress. *Nat. Neurosci.* **6**, 1100–1107 (2003).
27. Sahay, A. et al. Increasing adult hippocampal neurogenesis is sufficient to improve pattern separation. *Nature* **472**, 466–470 (2011).
28. Groves, J. O. et al. Ablating adult neurogenesis in the rat has no effect on spatial processing: evidence from a novel pharmacogenetic model. *PLoS Genet* **9**, e1003718 (2013).
29. Stenzel-Poore, M. P., Heinrichs, S. C., Rivest, S., Koob, G. F. & Vale, W. W. Overproduction of corticotropin-releasing factor in transgenic mice: a genetic model of anxiogenic behavior. *J. Neurosci.* **14**, 2579–2584 (1994).
30. Steffke, E. E., Kirca, D., Mazei-Robison, M. S. & Robison, A. J. Serum- and glucocorticoid-inducible kinase 1 activity reduces dendritic spines in dorsal hippocampus. *Neurosci. Lett.* **725**, 134909 (2020).
31. Tyan, S. W., Tsai, M. C., Lin, C. L., Ma, Y. L. & Lee, E. H. Serum- and glucocorticoid-inducible kinase 1 enhances zif268 expression through the mediation of SRF and CREB1 associated with spatial memory formation. *J. Neurochem* **105**, 820–832 (2008).
32. Yang, Y. C., Lin, C. H. & Lee, E. H. Serum- and glucocorticoid-inducible kinase 1 (SGK1) increases neurite formation through microtubule depolymerization by SGK1 and by SGK1 phosphorylation of tau. *Mol. Cell Biol.* **26**, 8357–8370 (2006).
33. Anacker, C. et al. Role for the kinase SGK1 in stress, depression, and glucocorticoid effects on hippocampal neurogenesis. *Proc. Natl Acad. Sci. USA* **110**, 8708–8713 (2013).
34. Licznerski, P. et al. Decreased SGK1 Expression and Function Contributes to Behavioral Deficits Induced by Traumatic Stress. *PLoS Biol.* **13**, e1002282 (2015).
35. Tsao, C.-H., Flint, J. & Huang, G.-J. Influence of diurnal phase on behavioral tests of sensorimotor performance, anxiety, learning and memory in mice. *Sci. Rep.* **12**, 432 (2022).

36. Chen, Y.-J. et al. Follistatin mediates learning and synaptic plasticity via regulation of Asic4 expression in the hippocampus. *Proc. Natl Acad. Sci.* **118**, e2109040118 (2021).
37. Huang, G.-J. et al. Neurogenomic evidence for a shared mechanism of the antidepressant effects of exercise and chronic fluoxetine in mice. *PloS One* **7**, e35901 (2012).

Acknowledgements

We would like to thank Dr. Andrew Edwards (Dykebar hospital, Scotland) for his helpful comments on this manuscript, NPAS Neuroscience Core Facility for technical support of electrophysiology (supported by grant No. AS-CFII-113-A6) and Dr. Li-Jen Lee (National Taiwan University, Taiwan) for providing the Neurolucida software. This study was supported by grants from the Chang Gung Memorial Hospital (CMRPD1M0832) and the National Science and Technology Council (112-2320-B-182-008-).

Author contributions

K-Y.W., C-H.T., and G-J.H. conceived the study. K-Y.W. and G-J.H. wrote the manuscript. K-Y.W. and C-H.T. conducted the histological and molecular biology experiments, and performed the animal behavioral assays with N.C.S.; S-M.D. performed Sholl analysis. All authors read and approved the final manuscript.

Competing interests

The authors declare no competing interests.

Additional information

Supplementary information The online version contains supplementary material available at https://doi.org/10.1038/s42003-025-08035-6.

Correspondence and requests for materials should be addressed to Guo-Jen Huang.

Peer review information *Communications Biology* thanks the anonymous reviewers for their contribution to the peer review of this work. Primary Handling Editors: Christoph Anacker and Laura Rodríguez Pérez.